Physica C 209 (1993) 585–590
North-Holland

PHYSICA C

# High-temperature resistivity and oxygen diffusion in $Bi_2Sr_2CaCu_2O_x$

S. McKernan and A. Zettl

*Department of Physics, University of California at Berkeley, and Materials Sciences Division, Lawrence Berkeley Laboratory, Berkeley, CA 94720, USA*

Received 25 January 1993

We have investigated high temperature electrical resistivity and oxygen diffusion in single crystal $Bi_2Sr_2CaCu_2O_x$. Above $\sim 400°C$, oxygen is readily exchanged with the sample environment which strongly influences the functional form of the resistivity. By changing the partial pressure of oxygen in the sample environment and by continuously monitoring the sample resistance at fixed temperature, we determine oxygen diffusion constants at selected temperatures. In-diffusion is found to be significantly faster than out-diffusion. The in-diffusion data suggest an activated form with a diffusion constant given by $D = D_0 \exp(-E/k_B T)$ with $D_0 = 11.7\ cm^2/s$ and $E = 1.16$ eV.

## 1. Introduction

It is well appreciated that oxygen content and ordering plays a central role in the normal and superconducting state properties of high-$T_c$ oxide superconductors. The 90 K superconductor $YBa_2Cu_3O_{7-\delta}$ (YBCO) has been perhaps the most studied material in this regard and numerous experiments have specifically addressed oxygen diffusion [1–3]. Early transport studies [4–6] of the related copper oxide $Bi_2Sr_2CaCu_2O_x$ (BSCCO) indicated that, for this material, the electronic and thermal properties are also extremely dependent on oxygen configuration. Other studies [7–9] have investigated in detail the relationship between oxygen content and normal-state resistivity and superconductivity in polycrystalline BSCCO.

In this communication, we report studies of the high temperature (25°C to 700°C) resistivity of single crystal BSCCO where the crystals are subjected to environments with varying oxygen concentration [5]. In- and out-diffusion of oxygen become appreciable above $\sim 400°C$, and the consequent variations in oxygen content of the specimens strongly affect the functional form of the temperature-dependent resistivity. Real-time experiments have been performed where the sample resistance is continuously monitored at fixed temperature as the environmental conditions are altered in a step-function fashion. The time evolution of the resistance allows oxygen diffusion constants to be determined directly. In-diffusion is found to be appreciably faster than out-diffusion. From temperature sweeps in fixed partial pressure oxygen environments, we also find that BSCCO crystals readily absorb oxygen from environmental concentrations of less than 0.1%.

## 2. Experimental technique

Single crystal samples of BSCCO were prepared in a melt reaction of high purity precursors using a method similar to that described previously [10]. Crystals were removed from the melt using adhesive tape and were subsequently cut to form long narrow bars for electrical resistance measurements. Typical dimensions of a cut sample were 1 mm × 250 μm × 50 μm. Samples were mounted on a quartz substrate with one mil gold four probe resistance leads attached using silver paint. In order to make robust contacts that could survive the high temperature oxidizing environment, many coats of progressively thicker silver paint were required. The quartz substrate and the BSCCO crystal were then mounted on an alumina probe in close proximity to a chromel/alumel thermocouple which was referenced to liquid

nitrogen. The four sample leads were attached to four ten mil gold wires which ran the length of the probe. The use of gold was necessitated by the oxidizing environment. At room temperature, typical two point contact resistances were under ten ohms while four point resistances were generally less than one ohm.

DC resistance measurements were made using a computer-controlled current source and voltmeter. The measurements were generally performed with no polarity reversal for subtraction of thermal EMFs. However, the reverse polarity resistance was periodically checked and found to be within 5% of the measured value. The oxygen concentration in the sample environment (1 atm pressure) was adjusted by mixing with argon. Concentrations were controlled using calibrated flowmeters. Temperature sweeps were performed from room temperature to 700°C.

## 3. Experimental results and discussion

Figure 1 shows the resistance of a single BSCCO crystal subjected to temperature cycling between room temperature and 700°C in the presence of either pure argon or pure oxygen. After an initial long high temperature anneal in argon, the crystal was cooled in argon to room temperature (curve 1). The sample was then warmed and cooled in a 100% oxygen environment (curves 2 and 3, respectively). Oxidation effects, that is, a decrease in resistance, are visible in curve 2 slightly above room temperature but do not really become substantial until the sample is above ~400°C.

Curve 3 in fig. 1 represents the "intrinsic" resistance for a "fully oxygenated" BSCCO crystal. From room temperature to about 250°C, the resistance is, to a good approximation, linear in temperature, consistent with other studies of polycrystalline [9] and crystalline [11] BSCCO. At higher temperatures, the resistance displays upward curvature. It seems inappropriate to associate this behavior with an unusual intrinsic scattering mechanism since the chemical composition of the sample here is changing with temperature; that is, even in a 1 atm 100% oxygen environment, oxygen is being depleted from the sample [5,9]. To extract the true functional form of

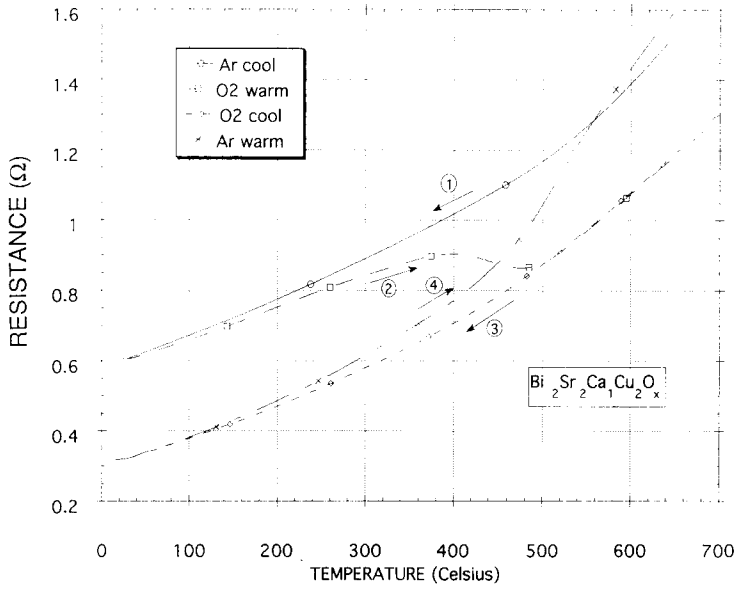


Fig. 1. Resistance vs. temperature for the cycling of a single crystal of BSCCO after a long-term high-temperature anneal of the sample in argon. The sample is first cooled in argon (curve 1) and then warmed (curve 2) and cooled (curve 3) in a 100% oxygen environment. Oxidation effects are clearly evident above 400°C. The final warming (curve 4) was done in argon with reduction not obvious until above 450°C.

the high temperature resistivity (which we expect to be linear even beyond 700°C) would necessitate control of the sample oxygen content (for example, by a high pressure oxygen environment).

The final argon warming plot in fig. 1 (curve 4) shows that deoxygenation of the crystal takes place over a larger temperature range than oxygenation (curve 2). Data similar to those shown in fig. 1 were obtained for oxygen concentrations varying from 100% (as in fig. 1) down to approximately 0.01%. Even at the lowest oxygen concentrations, oxidation effects were clearly visible after the high temperature argon anneal, and the curves were qualitatively the same as those in fig. 1. However, at the lowest oxygen concentrations (approximately 0.01%), the total resistive change between the argon and oxygen cycles fell to approximately 25% of the resistive difference reflected in fig. 1 (which is for 100% argon and 100% oxygen).

The data curves of fig. 1 were obtained using fairly slow temperature sweeps (typically many hours for one sweep). Faster sweeps resulted in qualitatively different curves especially at lower temperatures. These differences reflect fairly long timescales for oxygen diffusion into and out of the crystal. To investigate the timescale for diffusion directly, two different sets of experiments were performed. In the first, the sample was annealed for many hours in 100% argon. The sample environment was then changed to 100% oxygen in a step-function manner while maintaining a constant temperature. The sample resistance was continuously monitored. Essentially, this experiment determined the time evolution in dropping from curve 1 to curve 3 in fig. 1 at fixed temperature.

Figure 2 shows the results of the argon to oxygen environmental changes. The vertical arrows indicate the time at which the sample environment was changed from 100% argon to 100% oxygen (the absolute origin of the horizontal time axis is not significant). From fig. 2, it is apparent that oxygenation of the sample proceeds quite rapidly at high temperatures (less than 1 min at 700°C) and slowly at low temperatures (time constant on the order of 1 h at 420°C).

Figure 3 shows results for the second set of experiments in which the sample environment was altered in a step-function fashion from 100% oxygen

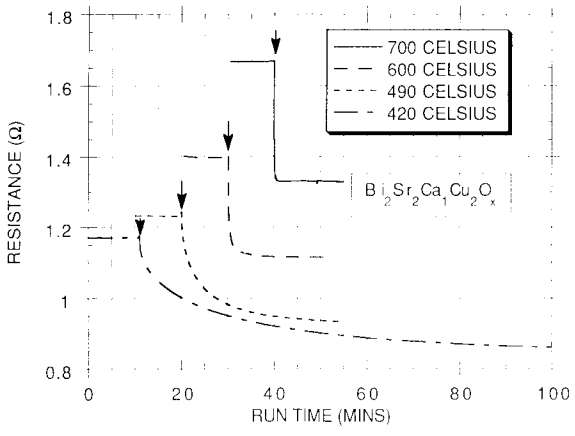


Fig. 2. Resistance vs. time for a single crystal of BSCCO with temperature constant at four temperatures. The exchange gas surrounding the sample is changed from argon to oxygen at the time indicated by the arrows. Sample oxidation is evident.

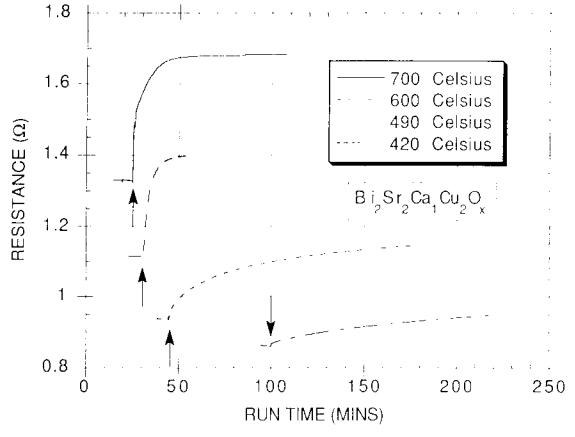


Fig. 3. Resistance vs. time for a single crystal of BSCCO with temperature constant at four temperatures. The exchange gas surrounding the sample is changed from oxygen to argon at the time indicated by the arrows. Reduction of the sample is evident.

to 100% argon. Again, the oxygen diffusion is more rapid at high temperature. However, the timescales for out-diffusion (fig. 3) are significantly longer than for in-diffusion (fig. 2). A direct comparison of the 700°C curves in figs. 2 and 3 is especially revealing: the time constant changes from less than 1 min for in-diffusion to approximately 20 min for out-diffusion. These differences correlate well with the data of fig. 1, where the sample appears to absorb oxygen

more easily at moderate temperature than lose it. A similar difference for out-diffusion and in-diffusion has been observed for YBCO [1,2].

The data of figs. 2 and 3 can be used to determine explicitly oxygen diffusion constants in BSCCO. We concentrate here on in-diffusion of oxygen. Since diffusion in the $a$–$b$ plane direction is expected to dominate $c$-axis diffusion, we assume a two-dimensional diffusion process. Furthermore, the large aspect ratio of the sample geometry allows us to neglect diffusion along the length of the crystal. Hence, we model the sample as a continuous set of resistors in parallel. We define $x$ to be orthogonal to the length of the sample, that is, along the path of diffusion with $x=0$ at the center line of the sample. The local resistivity at any point $x$ can then be written as

$$\rho(x)=\rho_0+\alpha\Phi(x,t), \tag{1}$$

where $\rho_0$ is the fully oxygenated sample resistivity, $\alpha$ is the change in resistivity between deoxygenated and oxygenated states, and $\Phi$ varies from zero to one to represent the sample deoxygenation level. With the above definition, $\Phi$ is zero everywhere for a fully oxygenated sample. For resistors in parallel, the total resistance can be found by summing the inverses of the individual resistors and inverting the sum

$$\frac{1}{R_{\text{tot}}}=\int\frac{d}{L\rho(x,t)}\,\mathrm{d}x \tag{2}$$

integrated from $-w/2$ to $w/2$, where $w$ is the width of the sample, $d$ is the sample thickness, and $L$ is the length of the sample between the voltage leads.

To obtain a functional form for $\rho(x,t)$, we combine the diffusion equation,

$$J=-D\nabla\Phi \tag{3}$$

with the continuity equation,

$$\nabla\cdot J=-\frac{\partial\Phi}{\partial t}, \tag{4}$$

which yields

$$\frac{\partial\Phi}{\partial t}=D\nabla^2\Phi. \tag{5}$$

This differential equation leads to a cosine dependence in $x$ and an exponential time dependence. $\Phi$ may be written in the following form

$$\Phi(x,t)=\sum A_i\cos(m_i x)\exp(-n_i t). \tag{6}$$

Substituting eq. (6) in (5), we find

$$n_i=Dm_i^2. \tag{7}$$

At time $t=0$, the oxygen is turned on, and the sample edges at $x=\pm w/2$ are immediately oxidized which implies $\Phi=0$ at the edges and $\Phi=1$ everywhere inside the sample. This leads to

$$m_i=\frac{(2i+1)\pi}{w}. \tag{8}$$

Multiplying both sides of eq. (6) with $\cos(mx)$ and integrating from 0 to $w/2$ we find

$$A_i=4\frac{(-1)^i}{(2i+1)\pi}. \tag{9}$$

Resubstituting the values found for $A_i$, $m_i$, and $n_i$ yields

$$\Phi(x,t)=\sum\frac{4(-1)^i}{(2i+1)\pi}\cos(m_i x)\exp(-Dm_i^2 t). \tag{10}$$

In order to simplify notation, we define the function

$$Q_i(t)=\frac{-D(2i+1)^2\pi^2 t}{w^2}. \tag{11}$$

Equation (2) now becomes

$$\frac{1}{R_{\text{tot}}}=2\int\mathrm{d}x\left\{\frac{d}{L(\rho_0+\alpha\sum A_i\cos(m_i x)Q_i(t))}\right\}. \tag{12}$$

This function has been summed, numerically integrated, and fit to the data using least squares by adjusting the value of the diffusion constant $D$. The in-diffusion data and the corresponding fits are shown in fig. 4. $\rho_0$ and $\alpha$ were adjusted for each fit using the data shown in fig. 1. The diffusion constant was found to be $D=1.30\times10^{-5}$ cm$^2$/s at 700°C, $2.23\times10^{-6}$ cm$^2$/s at 600°C, $1.81\times10^{-7}$ cm$^2$/s at 490°C, and $5.35\times10^{-8}$ cm$^2$/s at 420°C.

In fig. 5, we plot the diffusion constant values logarithmically versus $1/T$ with $T$ in K. We find that the data fit very well to an exponential dependence. The functional form of the temperature dependence of the diffusion constant is thus suggestive of the standard activated form

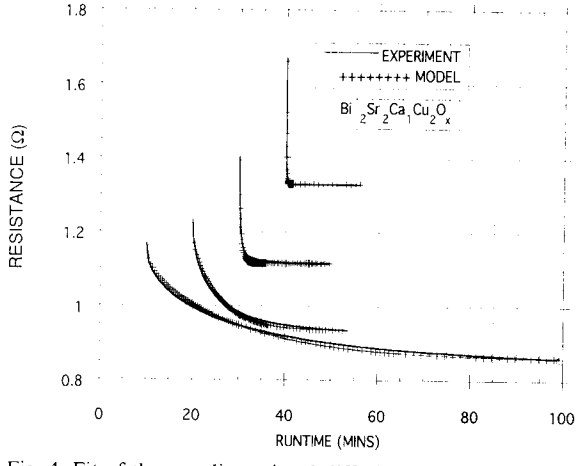


Fig. 4. Fit of the one-dimensional diffusion model to the data from fig. 2.

$$D = D_0 \, e^{-E/k_B T}, \tag{15}$$

with $D_0 = 11.7$ cm$^2$/s and $E = 1.16$ eV. This Arrhenius-type behavior has also been found in YBCO with the activation energy and diffusion coefficient in the same range as those found above [2,3].

## 4. Conclusion

We have studied the diffusion of oxygen in $Bi_2Sr_2CaCu_2O_x$ using in-situ resistometry at high temperature. It has been found that this material is very sensitive to oxygen, readily absorbing oxygen at concentrations of less than 0.1%. Using a simple anisotropic model for diffusion, oxygen in-diffusion constants have been extracted. The diffusion constant exhibits an Arrhenius-type behavior.

## Acknowledgements

We thank S. Hoen for help with the diffusion theory presented above, M. Crommie and G. Briceno for help in sample preparation, and M. Itzler for statistical help. This research was supported by National Science Foundation Grant No. DMR90-17254 and by the Director, Office of Energy Research, Office of Basic Energy Sciences, Materials Sciences Di-

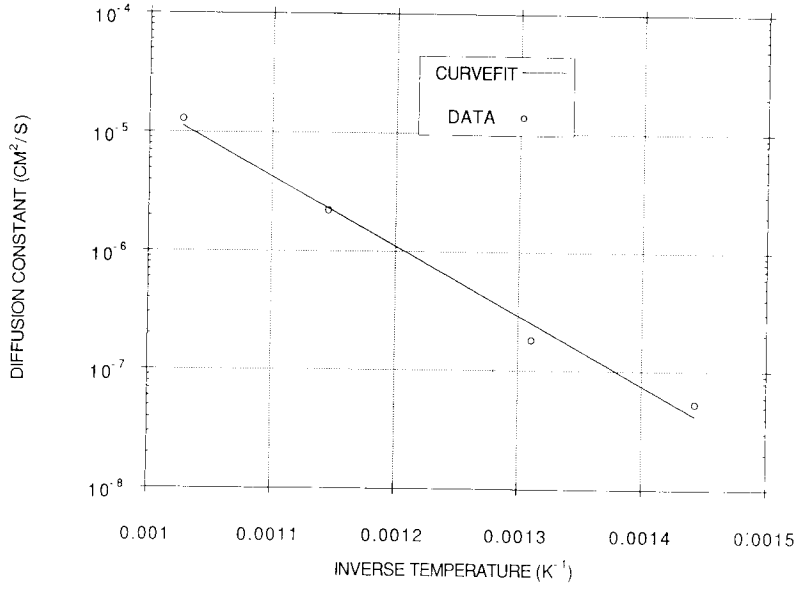


Fig. 5. A logarithmic plot of the experimentally determined diffusion constants vs. $1/T$. The plot suggests an activated behavior for the diffusion constant, $D = D_0 \exp(-E/k_B T)$.

vision of the US Department of Energy under Contract No. DE-AC03-76SF00098.

## References

[1] K.N. Tu, S.I. Park and C.C. Tsuei, Appl. Phys. Lett. 51 (1987) 2158.
[2] B.A. Glowacki, R.J. Highmore, K.F. Peters, A.L. Greer and J.E. Evetts, Supercond. Sci. Tech. 1 (1988) 7.
[3] K.N. Tu, N.C. Yeh, S.I. Park and C.C. Tsuei, Phys. Rev. B 38 (1988) 5118.
[4] M.F. Crommie, A.Y. Liu, M.L. Cohen and A. Zettl, Phys. Rev. B 41 (1990) 2526.
[5] H. Niu, N. Fukushima and K. Ando, Jpn. J. Appl. Phys. Lett. 27 (1988) L1442.
[6] L. Forro, J.R. Cooper, B. Leontic and B. Keszei, Europhys. Lett. 10 (1989) 371.
[7] H. Nagai, M. Kakuzen, M. Yokota and K. Majima, Jpn. J. Appl. Phys. Lett. 29 (1990) L1995.
[8] G. Triscone, J.-Y. Genoud, T. Graf, A. Junod and J. Muller, Physica C 176 (1991) 247.
[9] Y. Idemoto, S. Fujiwara and K. Fueki, Physica C 176 (1991) 325.
[10] J. Imer et al., Phys. Rev. Lett. 62 (1989) 336.
[11] S. Martin, A.T. Fiory, R.M. Fleming, L.F. Schneemeyer and J. V. Waszczak, Phys. Rev. Lett. 60 (1988) 2194.